THE JOURNAL OF PHYSICAL CHEMISTRY B LETTERS

2007, *111,* 12621−12624
Published on Web 10/13/2007

DFT Calculations on the Spin-Crossover Complex Fe(salen)(NO): A Quest for the Best Functional

Jeanet Conradie[†,‡] and Abhik Ghosh*[,†]

Department of Chemistry and Center for Theoretical and Computational Chemistry, University of Tromsø, N-9037 Tromsø, Norway, and Department of Chemistry, University of the Free State, 9300 Bloemfontein, Republic of South Africa

Received: June 9, 2007; In Final Form: September 18, 2007

DFT calculations on the spin-crossover complex Fe(salen)(NO) provide a striking illustration of the comparative performance of different exchange-correlation functionals vis-à-vis the issue of transition metal spin state energetics. Thus, although the "classic" pure functionals PW91 and BLYP favor the $S = {}^1/_2$ state by about 10 kcal/mol, relative to the $S = {}^3/_2$ state, the hybrid functional B3LYP favors the latter state by nearly the same margin. In contrast, the newer pure functionals OLYP and OPBE, based on the OPTX exchange functional, as well as the B3LYP* hybrid functional (which has 15% Hartree−Fock exchange, compared with 20% for B3LYP) predict nearly isoenergetic $S = {}^1/_2$ and ${}^3/_2$ states, as required for a spin-crossover complex. Intriguingly, the OLYP and B3LYP* spin density profiles for the $S = {}^1/_2$ state of Fe(salen)(NO) are substantially dissimilar.

For researchers involved in DFT calculations on open-shell transition metal complexes, including many important bioinorganic systems, a perennial question concerns the choice of the exchange-correlation functional.[1−3] Unfortunately, there have been only a few comparative studies of different functionals vis-à-vis the energetics of low-lying spin states of transition metal complexes.[4] Nevertheless, the limited amount of data suggests that, whereas "classic" pure functionals such as BLYP,[5,6] PW91,[7] and BP86[5,8] favor somewhat unduly spin-coupled, covalent descriptions, hybrid functionals such as B3LYP[9−11] err in the other direction. To correct for the latter tendency, the amount of Hartree−Fock exchange in B3LYP has been reduced from the standard 20% to 15%; the resulting B3LYP* functional has been found to yield improved results in certain cases.[12] These stereotypes of the different functionals were further confirmed in a recent study of first-row transition metal β-diketiminato (nacnac) imido complexes, where the classic pure functionals led to unduly low-multiplicity spin states, whereas the hybrid functionals B3LYP and O3LYP[13] resulted in unduly high-multiplicity ground states.[14] Interestingly, the OLYP[17] and OPBE[15,16] pure functionals, based on the new OPTX exchange functional,[17] yielded the correct ground states for all of the complexes examined, notably $S = 0$ for Co^{III}(nacnac)(NR) and $S = {}^3/_2$ for Fe^{III}(nacnac)(NR). This finding led us to speculate, albeit on the basis of a limited amount of data, that exchange-correlation functionals based on the OPTX-based exchange functional may be among the best from the point of view of transition metal spin state energetics.[14]

To further test this proposal, we carried out DFT calculations with different functionals on Fe(salen)(NO),[15] an archetypal spin-crossover complex. The question we sought to address in these calculations is: Which functional best reproduces isoenergetic $S = {}^1/_2$ and ${}^3/_2$ states for this complex? For comparison, we have also carried out a similar set of calculations on Fe(P)(NO) (P = porphyrin), which is expected to be $S = {}^1/_2$ like all {FeNO}[7] heme-NO derivatives,[18,19] and on Fe(5-Cl-salen)(NO), which has been found to be $S = {}^3/_2$.[20]

The $S = {}^1/_2$ and ${}^3/_2$ states of the above three molecules were optimized with the PW91[7] and OLYP[17,21] generalized gradient approximations (GGA), triple-ζ plus polarization Slater-type orbital basis sets, and a fine mesh for numerical integration of the matrix elements, as implemented in the ADF2006 program system.[22] In addition, two different C_s conformations A and B (see Figure 1) were optimized for Fe(salen)(NO) and Fe(5-Cl-salen)(NO). Subsequently, single-point BP86, BLYP, B3LYP, and B3LYP* calculations were carried out for the OLYP optimized geometries.[23] Figures 1, S1, and 2 present highlights of the OLYP results for Fe(salen)(NO), Fe(5-Cl-salen)(NO), and Fe(P)(NO), respectively. Tables 1−3 summarize the relative energetics of the different spin states and conformations studied. Similarly, Mulliken spin populations and charges for the two complexes are summarized in Tables 4, S1, and S2. Figure 3 presents a comparison of the PW91, OLYP, B3LYP*, and B3LYP spin density profiles for conformation A of $S = {}^1/_2$ Fe(salen)(NO). The highlights of our findings are as follows.

For Fe(salen)(NO) (see Table 1), the classic pure functionals PW91 and BLYP favor the $S = {}^1/_2$ state over the $S = {}^3/_2$ state by a large margin of about 10 kcal/mol. B3LYP, the paradigmatic hybrid functional, behaves oppositely, favoring the

* To whom correspondence should be addressed. E-mail: abhik@chem.uit.no.
[†] University of Tromsø.
[‡] University of the Free State.

10.1021/jp074480t CCC: $37.00

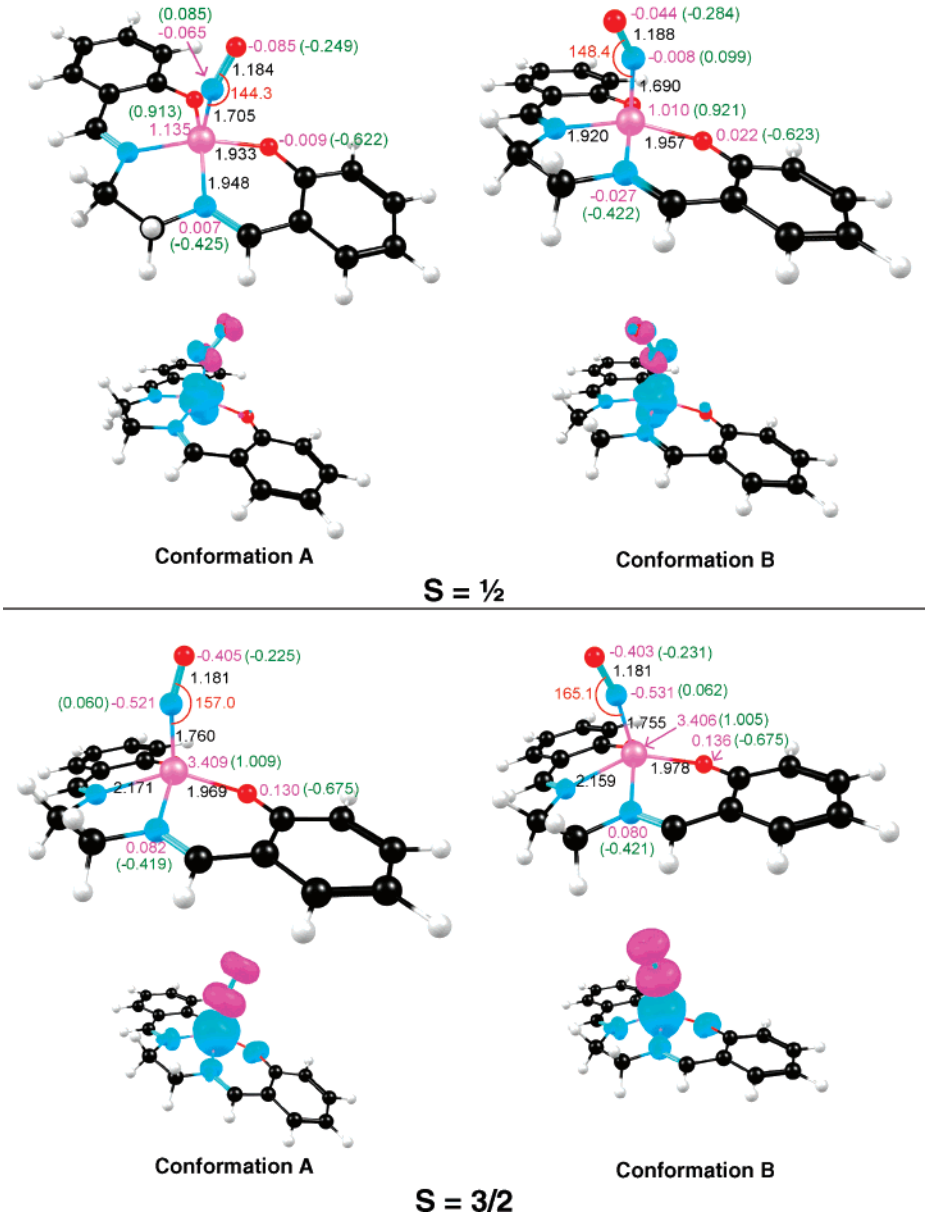

Figure 1. OLYP distances (Å, black), Mulliken charges (green), and spin populations (magenta). Majority and minority spin densities are plotted in cyan and magenta, respectively. Color code for atoms: C (black), H (white), N (magenta), O (red), Fe (cyan), and Cl (yellow).

$S = {}^3/_2$ state by about 9 kcal/mol. In contrast, OLYP and OPBE results in equienergetic $S = {}^1/_2$ and ${}^3/_2$ states, consistent with the observed spin-crossover behavior, whereas B3LYP* apparently also performs well exhibiting a slight preference for the $S = {}^3/_2$ state.

A similar state of affairs is found for Fe(5-Cl-salen)(NO) (see Table 2). However, here OLYP and OPBE still predict equienergetic $S = {}^1/_2$ and ${}^3/_2$ states, whereas B3LYP* favors the $S = {}^3/_2$ state by about 4 kcal/mol, i.e., by a slightly higher margin than in the case of Fe(salen)(NO). Given that Fe(5-Cl-salen)(NO) is in reality an $S = {}^3/_2$ species,[24] B3LYP* appears to do a better job of capturing the difference between salen and 5-Cl-salen, relative to OLYP.

For Fe(P)(NO) (see Table 3), the situation is qualitatively similar. Thus, although $\{FeNO\}^7$ heme-NO complexes invariably exhibit $S = {}^1/_2$ ground states, B3LYP predicts an $S = {}^3/_2$ ground state by a clear margin of energy! At the other extreme, the older pure functionals PW91 and BLYP favor the $S = {}^1/_2$ ground state by 15−20 kcal/mol. In contrast, OLYP and OPBE favor the $S = {}^1/_2$ state by about 6 kcal/mol, whereas B3LYP* favors the $S = {}^1/_2$ state by 2 kcal/mol. The results for Fe(salen)(NO), where the experimentally observed spin-crossover behavior provides a calibration of the calculated doublet-quartet splitting, add to growing evidence that OLYP and OPBE may be among the best functionals for transition metal spin state energetics.[14]

Before concluding, it is worth mentioning that the different functionals result in substantially different spin density profiles for the $S = {}^1/_2$ state of Fe(salen)(NO), although not for the $S = {}^3/_2$ state. For PW91 and BLYP, the Fe carries about 0.93 of an electron spin, whereas the NO nitrogen carries a spin population of only 0.03−0.04. For OLYP and OPBE, the Fe carries about 1.1−1.2 majority spins, whereas the NO carries about 0.1−0.2 minority spins. For B3LYP* and B3LYP, the Fe spin population is much higher—1.5 and 1.76, respectively—with correspondingly large minority spin populations on the NO. In other words, as we move from the classic pure functionals (PW91 and BLYP) through the newer OPTX-based pure functionals (OLYP and OPBE) to the hybrid functionals (B3LYP* and B3LYP), the spin density of the $S = {}^1/_2$ state becomes more and more like

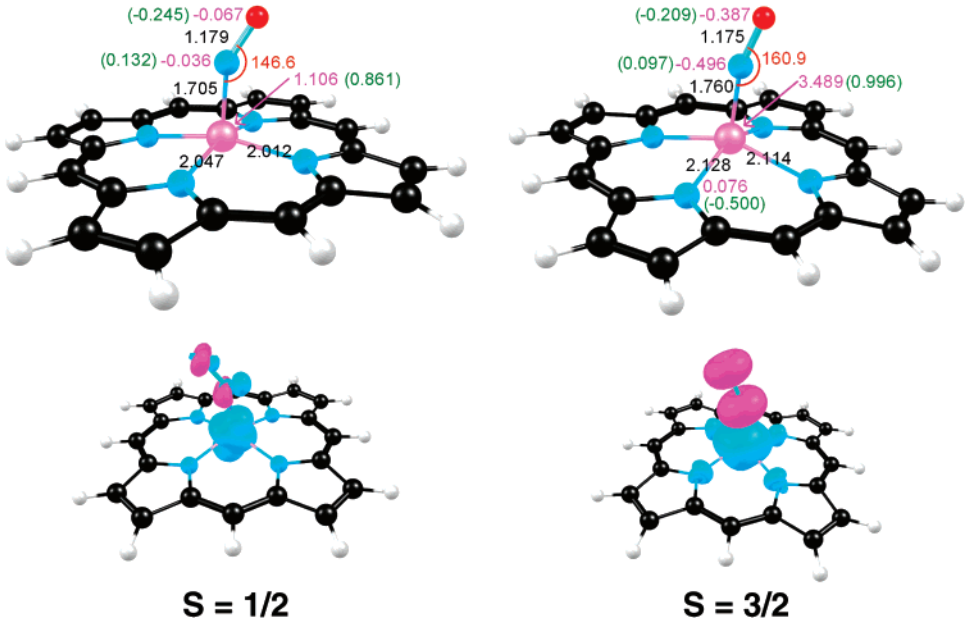

Figure 2. Calculated results for Fe(Por)(NO): OLYP optimized distances (Å, black), Mulliken charges (green), and spin populations (magenta). Majority and minority spin densities are plotted in cyan and magenta, respectively. Color code for atoms: same as in Figure 1.

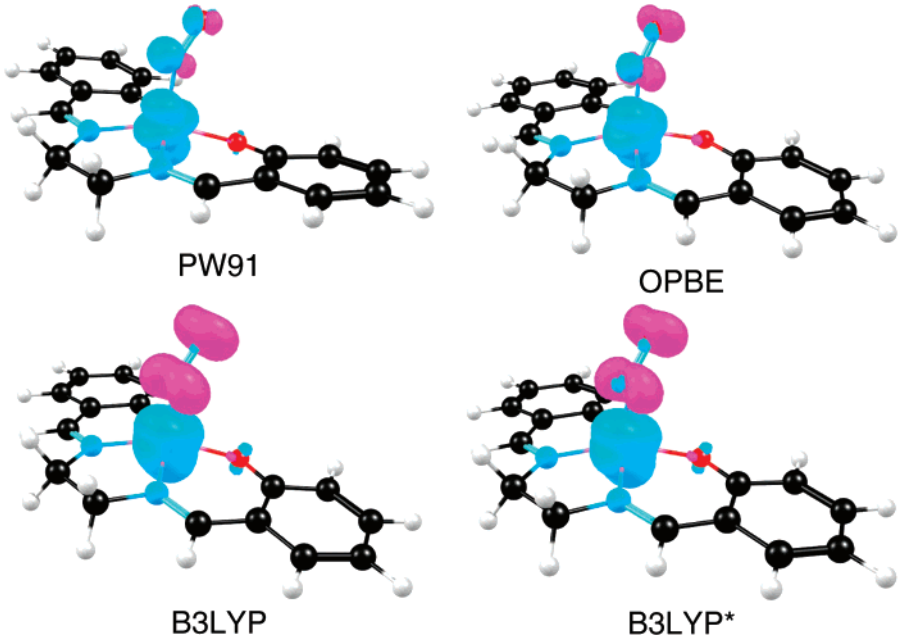

Figure 3. Spin density profiles of $S = {}^1/_2$ Fe(salen)(NO) (conformation A) for different functionals. Majority and minority spin densities shown in cyan and magenta, respectively. Color code for atoms: same as in Figure 1.

TABLE 1: Relative Energies (kcal/mol) of the Different Conformations and Spin States of Fe(salen)(NO)

		conformation A		conformation B	
functional	type of calculation	$S = {}^1/_2$	$S = {}^3/_2$	$S = {}^1/_2$	$S = {}^3/_2$
OLYP	geometry optimization	0.0	−1.2	−0.9	−0.5
PW91	geometry optimization	0.0	12.0	−1.6	10.8
OPBE	single-point	0.0	0.5	−1.2	0.9
BLYP	single-point	0.0	8.8	−0.2	9.5
B3LYP	single-point	0.0	−9.5	2.3	−8.8
B3LYP*	single-point	0.0	−3.5	0.7	−2.8

TABLE 2: Relative Energies (kcal/mol) of the Different Conformations and Spin States of Fe(5-Cl-salen)(NO)

		conformation A		conformation B	
functional	type of calculation	$S = {}^1/_2$	$S = {}^3/_2$	$S = {}^1/_2$	$S = {}^3/_2$
OLYP	geometry optimization	0.0	−0.9	−0.9	−0.7
PW91	single-point	0.0	13.8	1.2	13.8
OPBE	single-point	0.0	0.5	−1.4	0.5
BLYP	single-point	0.0	8.8	−0.5	9.0
B3LYP	single-point	0.0	−13.0	0.2	−13.0
B3LYP*	single-point	0.0	−4.4	0.5	−4.4

that expected of an intermediate-spin $S = {}^3/_2$ Fe(III) antiferromagnetically coupled to $S = 1$ NO^-. These dramatic variations in the $S = {}^1/_2$ spin density profile are graphically illustrated in Figure 3. In contrast, for the $S = {}^3/_2$ states, all of the functionals provide a qualitatively similar electronic description, involving a high-spin $S = {}^5/_2$ Fe(III) antiferromagnetically coupled to $S = 1$ NO^-, as has been found for variety of $S = {}^3/_2$ nonheme $\{FeNO\}^7$ complexes.[20,25]

TABLE 3: Relative Energies (kcal/mol) of the Different Spin States of Fe(Por)(NO)

functional	type of calculation	$S = {}^1/_2$	$S = {}^3/_2$
OLYP	geometry optimization	0.0	5.9
PW91	geometry optimization	0.0	18.9
OPBE	single-point	0.0	6.5
BLYP	geometry optimization	0.0	16.6
B3LYP	single-point	0.0	−4.6
B3LYP*	single-point	0.0	2.2

TABLE 4: Selected Mulliken Spin Populations (and Charges) for Different Conformations and Spin States of Fe(salen)(NO)

	$S = {}^1/_2$			$S = {}^3/_2$		
functional	Fe	N	O	Fe	N	O
			Conformation A			
OLYP	1.125	−0.065	−0.085	3.409	−0.521	−0.405)
	(0.913)	(0.085)	(−0.249)	(1.009)	(0.060)	(−0.225)
PW91	0.933	0.039	−0.004	3.131	−0.359	−0.299
	(0.809)	(0.111)	(−0.235)	(0.866)	(0.098)	(−0.213)
OPBE	1.179	−0.078	−0.093	3.463	−0.533	−0.407
	(0.897)	(0.092)	(−0.251)	(1.015)	(0.062)	(−0.229)
BLYP	0.927	0.034	−0.009	3.214	−0.421	−0.334
	(0.822)	(0.102)	(−0.234)	(0.884)	(0.089)	(−0.208)
B3LYP	1.755	−0.404	−0.363	3.728	−0.643	−0.540
	(1.002)	0.072)	(−0.254)	(1.100)	(0.043)	(−0.227)
B3LYP*	1.496	−0.262	−0.248	3.634	−0.607	−0.503
	(0.948)	(0.089)	(−0.245)	(1.045)	(0.056)	(−0.219)
			Conformation B			
OLYP	1.010	−0.008	−0.044	3.406	−0.531	−0.403
	(0.921)	(−0.099)	(−0.284)	(1.005)	(0.062)	(−0.231)
PW91	0.813	0.093	0.031	3.115	−0.358	−0.290
	(−0.274)	(0.122)	(−0.274)	(0.875)	(0.092)	(−0.231)
OPBE	1.050	−0.020	−0.051	3.459	−0.543	−0.405
	(0.906)	(0.106)	(−0.286)	(−0.235)	(0.065)	(−0.235)
BLYP	0.813	0.085	0.025	3.208	−0.428	−0.332
	(0.833)	(0.114)	(−0.269)	(0.885)	(0.088)	(−0.213)
B3LYP	0.525	0.294	0.167	3.727	−0.654	−0.533
	(0.983)	(0.126)	(−0.291)	(1.097)	(0.047)	(−0.236)
B3LYP*	1.337	−0.178	−0.179	3.632)	−0.617	−0.497
	(−0.284)	(0.107)	(−0.284)	(1.042	(0.060)	(−0.227)

In summary, the pure functionals OLYP and OPBE and the hybrid functional B3LYP* appear to provide the best spin-state energetics for the spin-crossover complex Fe(salen)(NO). Despite this similarity, OLYP (or OPBE) and B3LYP* provide significantly different spin density profiles, as described above.

Acknowledgment. This work was supported by the Research Council of Norway (A.G.) and the Central Research Fund of the University of the Free State (J.C.).

Supporting Information Available: Additional results and optimized coordinates (11 pages). This material is available free of charge via the Internet at http://pubs.acs.org.

References and Notes

(1) Ghosh, A.; Taylor, P. R. *Curr. Opin. Chem. Biol.* **2003**, *91*, 113−124.

(2) Harvey, J. N. *Struct. Bonding* **2004**, *112*, 151−183.

(3) Ghosh, A. *J. Biol. Inorg. Chem.* **2006**, *11*, 712−724.

(4) Selected studies comparing the performance of different functionals vis-à-vis transition metal spin state energetics: (a) Swart, M.; Groenhof, A. R.; Ehlers, A. W.; Lammertsma, K. *J. Phys. Chem. A* **2004**, *108*, 5479−5483. (b) Swart, M.; Ehlers, A. W.; Lammertsma, K. *Mol. Phys.* **2004**, *102*, 2467−2474. (c) Deeth, R. J.; Fey, N. *J. Comp. Chem.* **2004**, *25*, 1840−1848. (d) Groenhof, A. R.; Swart, M.; Ehlers, A. W.; Lammertsma, K. *J. Phys. Chem. A* **2005**, *109*, 3411−3417. (e) Daku, L. M. L.; Vargas, A.; Hauser, A.; Fouqueau, A.; Casida, M. E. *ChemPhysChem* **2005**, *6*, 1393−1410. (f) Ganzenmuller, G.; Berkaine, N.; Fouqueau, A.; Casida, M. E.; Reiher, M. *J. Chem. Phys.* **2005**, *122*, Art. No. 234321. (g) De Angelis, F.; Jin, N.; Car, R.; Groves, J. T. *Inorg. Chem.* **2006**, *45*, 4268−4276. (h) Vargas, A.; Zerara, M.; Krausz, E.; Hauser, A.; Daku, L. M. L. *J. Chem. Theory Comput.* **2006**, *2*, 1342−1359. (i) Rong, C. Y.; Lian, S. X.; Yin, D. L.; Shen, B.; Zhong, A. G.; Bartolotti, L.; Liu, S. B. *J. Chem. Phys.* **2006**, *125*, Art. No. 174102. (j) Strickland, N.; Harvey, J. N. *J. Phys. Chem. B* **2007**, *111*, 841−852.

(5) Becke, A. D. *Phys. Rev.* **1988**, *A38*, 3098.

(6) Lee, C., Yang, W., Parr, R. G. *Phys. Rev.* **1988**, *B37*, 785−789.

(7) Perdew, J. P.; Chevary, J. A.; Vosko, S. H.; Jackson, K. A.; Perderson, M. R.; Singh, D. J.; Fiolhais, C. *Phys. Rev. B* **1992**, *46*, 6671−6687. Erratum: Perdew, J. P.; Chevary, J. A.; Vosko, S. H.; Jackson, K. A.; Perderson, M. R.; Singh, D. J.; Fiolhais, C. *Phys. Rev. B* **1993**, *48*, 4978.

(8) Perdew, J. P. *Phys. Rev.* **1986**, *B33*, 8822. Erratum: Perdew, J. P. *Phys. Rev.* **1986**, *B34*, 7406.

(9) Stephens, J.; Devlin, F. J.; Chabalowski, C. F.; Frisch, M. J. *J. Phys. Chem.* **1994**, *98*, 11623−11627.

(10) Watson, M. A.; Handy, N. C.; Cohen, A. J. *J. Chem. Phys.* **2003**, *119*, 6475−6481.

(11) Hertwig, R. H.; Koch, W. *Chem. Phys. Lett.* **1997**, *268*, 345−351.

(12) Reiher, M.; Salomon, O.; Hess, B. A. *Theor. Chem. Acc.* **2001**, *107*, 48.

(13) Cohen, A. J.; Handy, N. C. *Mol. Phys.* **2001**, *99*, 607−615.

(14) Conradie, J.; Ghosh, A. *J. Chem. Theory Comput.* **2007**, *3*, 689−702.

(15) Perdew, J. P.; Burke, K.; Ernzerhof, M. *Phys. Rev. Lett.* **1996**, *77*, 3865−3868.

(16) Perdew, J. P.; Burke, K.; Ernzerhof, M. *Phys. Rev. Lett.* **1997**, *78*, 1396.

(17) Handy, N. C.; Cohen, A. J. *Mol. Phys.* **2001**, *99*, 403−412.

(18) For a review of DFT calculations on metalloporphyrin−NO complexes, see: Ghosh, A. *Acc. Chem. Res.* **2005**, *38*, 943−954.

(19) The superscript 7 in $\{FeNO\}^7$ refers to Enemark−Feltham electron count, defined as the sum of the numbers of metal d and NO π^* electrons: Westcott, B. L.; Enemark, J. L. In *Inorganic Electronic Structure and Spectroscopy*; Solomon, E. I., Lever, A. B. P., Eds.; Wiley: New York, 1999; Vol. 2, pp 403−450.

(20) Selected DFT calculations on nonheme $\{FeNO\}^7$ complexes: (a) Brown, C. A.; Pavovski, M. A.; Westre, T. E.; Zhang, Y.; Hedman, B.; Hodgson, K. O.; Solomon, E. I. *J. Am. Chem. Soc.* **1995**, *117*, 715−732. (b) Schenk, G.; Pau, M. Y. M.; Solomon, E. I. *J. Am. Chem. Soc.* **2004**, *126*, 505−515. (c) Rodriguez, J. H.; Xia, Y.-M.; Debrunner, P. G. *J. Am. Chem. Soc.* **1999**, *121*, 7846−7863. (d) Zhang, Y.; Oldfield, E. *J. Am. Chem. Soc.* **2004**, *126*, 9494−9495. (e) Zhang, Y.; Oldfield, E. *J. Phys. Chem. A* **2003**, *107*, 4147−4150. (f) Cheng, H.-Y.; Chang, S. *Int. J. Quantum Chem.* **2005**, *105*, 511−517. (g) Li, M.; Bonnet, D.; Bill, E.; Neese, F.; Weyhermuller, T.; Blum, N.; Sellman, D.; Wieghardt, K. *Inorg. Chem.* **2002**, *41*, 3444−3456. (h) Serres, R. G.; Grapperhaus, C. A.; Bothe, E.; Bill, E.; Weyhermuller, T.; Neese, F.; Wieghardt, K. *J. Am. Chem. Soc.* **2004**, *126*, 5138−5153.

(21) The LYP correlation functional: Lee, C.; Yang, W.; Parr, R. G. *Phys. Rev. B* **1988**, *37*, 785−789.

(22) The ADF program system was obtained from Scientific Computing and Modeling, Amsterdam (http://www.scm.com/). For a description of the methods used in ADF, see: Velde, G. T.; Bickelhaupt, F. M.; Baerends, E. J.; Guerra, C. F.; Van Gisbergen, S. J. A.; Snijders, J. G.; Ziegler, T. *J. Comput. Chem.* **2001**, *22*, 931−967.

(23) The assumption here is that the geometries of the molecules studied are largely independent of the functional. This is widely recognized to be the case by the DFT community. To quote a recent review on DFT caculations on bioinorganic systems (Neese, F. *J. Biol. Inorg. Chem.* **2006**, *11*, 702−711), "Geometries predicted by DFT methods tend to be quite reliable. Moreover, the predicted geometries converge quickly with basis set size.... Different DFT functionals behave quite similarly as long as at least gradient corrections are taken into account (e.g. one has to go beyond the local density approximation, LDA)".

(24) Wells, F. V.; McCann, S. W.; Wickman, H. H.; Kessel, S. L.; Hindrickson, D. N.; Feltham, R. D. *Inorg. Chem.* **1982**, *21*, 2306−2311.

(25) Conradie, J.; Quarless, D. A., Jr.; Hsun, H.-F.; Harrop, T. C.; Lippard, S. J.; Koch, S. A.; Ghosh, A. *J. Am. Chem. Soc.* **2007**, *129*, 10446−10456.